

**Running Head: CYP71D351 catalyzes tabersonine 16-hydroxylation**

**Corresponding author:** Vincent Courdavault

Université François-Rabelais de Tours - EA 2106 "Biomolécules et Biotechnologies  
Végétales", UFR des Sciences et Techniques, 37200, Tours, France

Phone: +33 247 36 70 23; Fax: +33 247 27 66 60

e-mail: [vincent.courdavault@univ-tours.fr](mailto:vincent.courdavault@univ-tours.fr)

**Research Area:** Biochemistry and Metabolism

## **A pair of tabersonine 16-hydroxylases initiates the synthesis of vindoline in an organ dependent manner in *Catharanthus roseus***

Sébastien Besseau<sup>1\*</sup>, Franziska Kellner<sup>2\*</sup>, Arnaud Lanoue<sup>1</sup>, Antje MK Thamm<sup>3</sup>, Vonny Salim<sup>3</sup>, Bernd Schneider<sup>4</sup>, Fernando Geu-Flores<sup>2</sup>, René Höfer<sup>5</sup>, Grégory Guirimand<sup>1</sup>, Anthony Guihur<sup>1</sup>, Audrey Oudin<sup>1</sup>, Gaëlle Glevarec<sup>1</sup>, Emilien Foureau<sup>1</sup>, Nicolas Papon<sup>1</sup>, Marc Clastre<sup>1</sup>, Nathalie Giglioli-Guivarc'h<sup>1</sup>, Benoit St-Pierre<sup>1</sup>, Danièle Werck-Reichhart<sup>5</sup>, Vincent Burlat<sup>6, 7</sup>, Vincenzo De Luca<sup>3</sup>, Sarah O'Connor<sup>2</sup>, Vincent Courdavault<sup>1#</sup>

\*Both authors have contributed equally to this work

#corresponding author

<sup>1</sup>Université François Rabelais de Tours, EA2106 "Biomolécules et Biotechnologies Végétales"; 37200 Tours, France

<sup>2</sup>Department of Biological Chemistry, John Innes Centre, Norwich Research Park, Colney, Norwich NR4 7UH, United Kingdom

<sup>3</sup>Department of Biological Sciences, Brock University, 500 Glenridge Avenue, St Catharines, Ontario, L2S 3A1, Canada

<sup>4</sup>Max-Planck-Institute for Chemical Ecology, Beutenberg Campus, Hans-Knöll-Str. 8, D-07745 Jena, Germany

<sup>5</sup>Institut de Biologie Moléculaire des Plantes, Unité Propre de Recherche 2357 du Centre National de la Recherche Scientifique, University of Strasbourg, 28 Rue Goethe, F-67083 Strasbourg Cedex, France

<sup>6</sup>Université de Toulouse ; UPS ; UMR 5546, Laboratoire de Recherche en Sciences végétales ; BP 42617 Auzeville, F-31326, Castanet-Tolosan, France

<sup>7</sup>CNRS; UMR 5546; BP 42617, F-31326, Castanet-Tolosan, France

**One-sentence summary:** A newly identified cytochrome P450 isoform initiates the synthesis of valuable alkaloids in leaves of *Catharanthus roseus* by hydroxylating tabersonine.

**Footnotes:** This work was supported by the “Ministère de l’Enseignement Supérieur et de la Recherche” (MESR), by a grant from the University of Tours (SB, AL, GrG, AG, AO, GaG, EF, NP, MC, NGG, BSt-P, VC), by the BBSRC (BB/J004561/1 and BB/J009091/1- FK, FGF, SOC) and by the “National Science and Engineering Research Council of Canada Discovery Grants” (AT, VS, VDL).

**Abstract:**

Hydroxylation of tabersonine at the C-16 position, catalyzed by tabersonine 16-hydroxylase (T16H), initiates the synthesis of vindoline that constitutes the main alkaloid accumulated in leaves of *Catharanthus roseus*. Over the last decade, this reaction has been associated with CYP71D12 cloned from undifferentiated *C. roseus* cells. In the present study, we isolated a second cytochrome P450 (CYP71D351) displaying T16H activity. Biochemical characterization demonstrated that CYP71D12 and CYP71D351 both exhibit high affinity for tabersonine and narrow substrate specificity, making of T16H the first alkaloid biosynthetic enzyme displaying two isoforms encoded by distinct genes, characterized to date in *C. roseus*. However, both genes dramatically diverge in transcript distribution *in planta*. While *CYP71D12* (T16H1) expression is restricted to flowers and undifferentiated cells, *CYP71D351* (T16H2) expression profile is similar to the other vindoline biosynthetic genes reaching a maximum in young leaves. Moreover, transcript localization by carborundum abrasion and RNA *in situ* hybridization demonstrated that *CYP71D351* mRNA are specifically located to leaf epidermis, which also host the next step of vindoline biosynthesis. Comparison of high and low vindoline accumulating *C. roseus* cultivars also highlights the direct correlation between *CYP71D351* transcript and vindoline levels. In addition, *CYP71D351* down-regulation mediated by virus-induced gene silencing reduces vindoline accumulation in leaves and re-directs the biosynthetic flux towards the production of unmodified alkaloids at the C-16 position. All these data demonstrate that tabersonine 16-hydroxylation is orchestrated in an organ-dependent manner by two genes including *CYP71D351* that encodes the specific T16H isoform acting in the foliar vindoline biosynthesis.

## **INTRODUCTION**

*Catharanthus roseus* (Madagascar periwinkle) displays an active specialized metabolism producing more than one hundred monoterpene indole alkaloids (MIAs). MIAs are a major component of the chemical arsenal that likely protects the plant by acting against herbivores (Guirimand et al., 2010a; Roepke et al., 2010). These MIAs include highly valuable molecules that exhibit interesting pharmacological properties for human health. For instance, vinblastine, vincristine and their derivatives are widely used in cancer chemotherapy, where they act as microtubule disruptors (Gigant et al., 2005). Due to highly complex structures, these therapeutic molecules are prepared by semi-synthesis using natural precursors extracted from *C. roseus* leaves. Their extremely low level *in planta* explains their high cost of production and justifies the extensive study of the MIA biosynthetic pathway that has been carried out over the last three decades, making of *C. roseus* one of the most studied plants for specialized metabolism (Facchini and De Luca, 2008; Guirimand et al., 2010b).

Vinblastine and vincristine are dimeric MIAs resulting from the oxidative coupling of two monomeric precursors, catharanthine (*Iboga* MIA) and vindoline (*Aspidosperma* MIA), which constitute the major MIAs that accumulate in *C. roseus* leaves as compared to the trace amounts of dimeric MIAs (Westekemper et al., 1980). Vindoline as well as dimeric MIAs are restricted to aerial organs such as leaves and stems, while catharanthine is accumulated equally throughout under- and above-ground organs (Deus-Neumann et al., 1987; Balsevich and Bishop, 1989) with a specific secretion of this MIA in leaf wax exudates (Roepke et al., 2010). In contrast to the limited available data regarding catharanthine biosynthesis, characterization of the *in folio* vindoline biosynthetic pathway is now approaching completion (**Fig. 1**). This pathway relies on a six-step conversion of tabersonine initiated by tabersonine 16-hydroxylase (T16H; EC 1.14.13.73), which is a cytochrome P450 (P450) that hydroxylates tabersonine at the 16 position (St-Pierre and De Luca, 1995). Accumulating evidence argues for a key role of T16H in vindoline biosynthesis, since for instance, screening of low and high MIA-accumulating cultivars of *C. roseus* revealed a direct correlation of vindoline content with T16H activity (Magnotta et al., 2006). After hydroxylation, the resulting 16-hydroxytabersonine is successively *O*-methylated by 16-hydroxytabersonine 16-*O*-methyltransferase (16OMT; Levac et al., 2008), reduced at the C2-C3 double bond with concomitant hydroxylation at the C-3 position through an uncharacterized mechanism of hydration, and *N*-methylated at the indolic nitrogen by 16-methoxy-2,3-dihydro-3-hydroxytabersonine *N*-methyl transferase (NMT; De Luca et al., 1987; Liscombe et al., 2010)

to form desacetoxyvindoline. The last two steps of this pathway involve an additional hydroxylation catalyzed by desacetoxyvindoline-4-hydroxylase (D4H, Vazquez-Flota et al., 1997) and a final *O*-acetylation performed by deacetylvindoline-4-*O*-acetyltransferase (DAT, St-Pierre et al., 1998) leading to the formation of vindoline. In roots, the fate of tabersonine is different and relies on its conversion into hörhammericine and echitovenine, where a recently characterized cytochrome P450, CYP71BJ1, acts as 19-hydroxylase (Giddings et al., 2011) and a minovincinine-*O*-acetyltransferase (MAT; Laflamme et al., 2001) closely related to DAT catalyze the subsequent reaction (**Fig. 1**).

The vindoline biosynthetic pathway displays a high degree of compartmentalization of both gene expression and enzymatic reactions, especially in *C. roseus* leaves. While transcripts and enzyme activities of both D4H and DAT have been localized to laticifers/idioblasts, adaxial and abaxial epidermal cells have been shown to host the starting steps of the biosynthetic pathway. The epidermal localization of *16OMT* transcripts was first established using epidermis-specific mRNA enrichment procedures performed by carborundum abrasion or epidermis laser-capture microdissection/EST sequencing (Murata and De Luca, 2005; Levac et al., 2008; Murata et al., 2008) and was further confirmed by RNA *in situ* hybridization (Guirimand et al., 2011a). By contrast, the situation is less clear for T16H, whose only known coding sequence, *CYP71D12*, was cloned from *C. roseus* cell cultures (Schröder et al., 1999, Guirimand et al., 2011a). Evidence of the leaf epidermal localization of *T16H* transcripts was initially obtained by RT-PCR procedures and epidermis EST sequencing (Murata and De Luca, 2005; Murata et al., 2008). However, all our attempts to confirm these results by RNA *in situ* hybridization failed. This is surprising considering that the frequency of ESTs annotated as *T16H* in the *C. roseus* epidermome is similar or higher to those of other MIA biosynthetic genes such as strictosidine synthase (*STR*) and strictosidine  $\beta$ -D-glucosidase (*SGD*), both of which have previously been localized in leaf epidermis using RNA *in situ* hybridization (St-Pierre et al., 1999, Murata et al., 2008, Guirimand et al., 2010a). This discrepancy prompted us to investigate the 16-hydroxylation of tabersonine in more detail and led to the identification of a second cytochrome P450 displaying T16H activity, CYP71D351. Comparative expression analysis of CYP71D351 and CYP71D12, cellular transcript distribution as well as gene silencing in seedlings allowed us to conclude that the newly discovered CYP71D351, and not the previously cloned CYP71D12, initiates vindoline biosynthesis in *C. roseus* leaves. In contrast, CYP71D12 appears to be dedicated to vindoline biosynthesis in flowers.

## **RESULTS**

### ***Isolation of CYP71D351 cDNA***

While the coding sequence of the original full-length T16H (*CYP71D12*, Genbank accession number FJ647194) could be efficiently amplified by PCR using cDNAs prepared from *C. roseus* cell cultures (Guirimand et al., 2011a), all our attempts to carry out this amplification using reverse-transcribed RNAs extracted from young leaves failed. As a consequence, additional amplifications of a partial internal sequence were attempted using young leaf cDNAs and the previously described CrT16H-RT01 and CrRT16H-RT02 primers (Murata and De Luca, 2005). This allowed obtaining a unique 242-bp cDNA fragment that displays 96% identity with the corresponding region of the *CYP71D12* coding sequence (**Supplemental Fig. 1**). By combining 5' and 3' RACE with EST database analysis, we amplified a 1698 bp-long cDNA that encompassed a 1539-bp open reading frame 86.5% identical to that of the *CYP71D12* nucleic acid sequence. Interestingly, we noted that all four *T16H*-annotated ESTs identified within the *C. roseus* epidermome EST database were strictly identical to the new amplified cDNA and slightly different from *CYP71D12* (Murata et al., 2008, **Supplemental Table 1**). The encoded 512-amino acid protein, which is 82% identical to *CYP71D12* (**Supplemental Fig. 2**), was named CYP71D351 according to the standardized system of P450 nomenclature (Nelson, 2006). By contrast, CYP71D351 displays only low amino acid identity with other P450s associated with MIA biosynthesis such as secologanin synthase (*CYP72A1*; 20%), geraniol 10-hydroxylase (*CYP76B6*; 33%) or the recently characterized tabersonine 19-hydroxylase (*CYP71BJ1*; 35%).

### ***CYP71D351 catalyzes the 16-hydroxylation of tabersonine***

To analyze the activity of CYP71D351, both *CYP71D12* (the gene originally assigned as T16H) and CYP71D351 were individually expressed in *S. cerevisiae* WAT11 strain, a yeast strain engineered for plant P450 protein studies via the co-expression of the *Arabidopsis* NADPH P450 Reductase 1 (Pompon et al., 1996). While microsomes of the control yeast strain (carrying the empty expression vector) did not metabolize tabersonine, LC-MS and GC-MS analysis revealed that microsomes of both strains expressing the cytochrome P450s could convert tabersonine into a more hydrophilic compound displaying a retention time and a mass-to-charge ratio consistent with hydroxylated tabersonine (**Figure 2A**; **Supplemental Figure 3**). No enzymatic products were observed when NADPH was omitted from the reactions, confirming that the hydroxylation occurred in a NADPH-dependent manner, as

previously described for CYP71D12 (St-Pierre and De Luca, 1995; Schröder et al., 1999). To investigate the position at which CYP71D351 was hydroxylating tabersonine, the enzymatic product from a large-scale reaction was purified and analyzed by  $^1\text{H}$  NMR,  $^1\text{H}$ - $^1\text{H}$  COSY, HSQC and HMBC NMR. The  $^{13}\text{C}$  NMR chemical shifts of the new metabolite, which were obtained from the HSQC and HMBC spectra, were similar to the ones reported previously for 16-hydroxytabersonine (He et al., 1994). Notably, in comparison to the  $^{13}\text{C}$  NMR spectra reported for tabersonine (Wenkert et al., 1973), the signal from C-16 was shifted to lower field (from  $\delta$  127.6 to  $\delta$  160.6), while the signals from C-15 and C-17 were shifted to higher field (from  $\delta$  120.5 to  $\delta$  108.7, and from  $\delta$  109.2 to  $\delta$  99.6, respectively), clearly indicating an electronegative substituent, such as a hydroxyl group, at C-16. Also importantly, the three-spin system of H-14 ( $\delta$  7.32, d,  $J$  = 8.1 Hz), H-15 ( $\delta$  6.37, dd,  $J$  = 8.1, 2.1 Hz), and H-17 ( $\delta$  6.53, d,  $J$  = 2.1 Hz) and their HMBC correlations through three bonds (H-14  $\rightarrow$  C-12, C-16, C-18; H-15  $\rightarrow$  C-13, C-17; H-17  $\rightarrow$  C-13, C-15) confirmed the hydroxyl transfer at the C16 position of the aromatic ring (**Fig. 2B**). All these results demonstrate that CYP71D351 catalyzes the 16-hydroxylation of tabersonine and in turn prove the existence of two T16H isoforms in *C. roseus*. Therefore, we propose to extend the T16H nomenclature and to annotate CYP71D12 and CYP71D351 as T16H1 and T16H2, respectively.

### ***Enzyme kinetic parameters***

Both CYP71D12- and CYP71D351-enriched yeast microsomes were incubated with varying amounts of tabersonine to compare the kinetic parameters of the two enzymes (**Supplemental Figure 4**). CYP71D12 (T16H1) displayed an apparent  $K_m$  of  $350 \pm 100$  nM and  $V_{max}$  of  $1.8 \pm 0.05$   $\mu\text{M min}^{-1}$ . Interestingly, these values are of the same magnitude as those reported for T19H but much lower than the  $K_m$  for tabersonine evaluated using a T16H/16OMT coupled system (11  $\mu\text{M}$ ) (St-Pierre and De Luca, 1995, Giddings et al., 2011). By contrast, CYP71D351 (T16H2) exhibited a lower apparent  $K_m$  of  $70 \pm 20$  nM and a  $V_{max}$  of  $2.2 \pm 0.25$   $\mu\text{M min}^{-1}$ . This difference in apparent  $K_m$  suggests that this new isoform has a higher affinity for tabersonine than CYP71D12.

### ***Substrate specificity analysis***

To analyze the substrate specificity of CYP71D351 and CYP71D12, microsomes from yeast strains expressing each enzyme were assayed against several different compounds including MIAs, MIA precursors, and naringenin, which is an hydroxylatable flavonoid with aromatic ring, accumulated in leaf epidermis and substrate of geraniol 10-hydroxylase (Sung et al.,



2011). LC-MS analysis of reaction mixtures revealed that, among all the tested compounds, only tabersonine (*Aspidosperma* MIA) and to a lesser extent the two closely related compounds, 2,3-dihydro-3-hydroxytabersonine and 2,3-dihydrotabersonine, were metabolized by the two enzymes (**Table 1**). Interestingly, while hydroxylation of these last two compounds by CYP71D12 (T16H1) occurred at very low levels, CYP71D351 (T16H2) was more permissive towards these substrates. The lack of hydroxylating activity towards the other substrates tested, including naringenin, suggests that both CYP71D351 and CYP71D12 are specific enzymes acting *in vivo* in the conversion of tabersonine to 16-hydroxytabersonine in the vindoline pathway.

### **CYP71D351 (T16H2) and CYP71D12 (T16H1) display different transcript distributions in *C. roseus***

The identification of a second T16H isoform prompted us to investigate the distribution of *CYP71D351* and *CYP71D12* transcripts in *C. roseus* plant organs and cell cultures. Since *CYP71D12* (T16H1) was initially isolated from *C. roseus* cell cultures, we first analyzed transcript levels of both enzymes in this system by quantitative real-time PCR. As expected, *CYP71D12* transcripts were easily detectable in cell cultures and were responsive to methyl jasmonate (MeJa) treatment, as previously reported (Schröder et al., 1999; He et al., 2011) (**Fig. 3A**). By contrast, transcripts of *CYP71D351* (T16H2) were barely detectable (approximately 100- to 1000-fold less abundant) and exhibited a weak response to MeJa treatment, suggesting that the T16H activity previously measured in cell cultures resulted mainly from CYP71D12 (Schröder et al., 1999). The situation was strikingly different in whole plants (Pacifica Pink cultivar), given that the *CYP71D12* expression level was extremely low in most of the tested organs (**Fig. 3B**). *CYP71D12* transcripts were barely detectable or undetectable in roots, internodes, young and mature leaves, and flower buds, but were relatively abundant in fully developed flowers. The expression pattern of *CYP71D351* was strikingly dissimilar, including very low transcript levels in roots and fruits, low levels in stem, flower buds and flowers, and very high amounts in leaves, especially young leaves, where the highest levels of T16H enzymatic activity have been found (St-Pierre and De Luca, 1995). In this organ, *CYP71D351* transcript level was also dramatically higher than the amount of *CYP71D12* transcripts, which just reached the level of detection. These results suggest that CYP71D351 (T16H2) has a major role in the biosynthesis of vindoline in leaves, while CYP71D12 (T16H1) may play an analogous role in flowers, where vindoline does accumulate, albeit at lower levels (**Supplemental Figure 5**).

### ***CYP71D351 (T16H2) expression follows the expression of other vindoline biosynthetic genes***

The specific distribution of *CYP71D12* and *CYP71D351* transcripts was also compared to that of other known vindoline biosynthetic pathway genes, including *16OMT*, *NMT* and *DAT* together with *MAT*, which catalyzes the penultimate step in the biosynthesis of echitovenine in roots (Laflamme et al., 2001). As depicted in **Fig. 4**, *CYP71D351 (T16H2)* displayed the same pattern of expression as *16OMT*, *NMT* and *DAT*, including highest transcript amounts in young leaves, lower level in mature leaves and in flower buds, and very low levels in roots, stem, flowers and fruits. This contrasts with the expression profile of *MAT*, which had the highest mRNA levels in roots, consistent with its role in echitovenine/hörhammericine biosynthesis. In addition, *CYP71D12 (T16H1)* displayed an expression profile that was very different from the characteristic profile of the known vindoline biosynthetic genes. These expression profiles argue in favor of the involvement of *CYP71D351* in leaf vindoline biosynthesis.

### ***CYP71D351 (T16H2) transcripts are localized in the epidermis of C. roseus leaves***

Previous work suggested an epidermis specific localization of *CYP71D12 (T16H1)* transcripts in leaf (Murata and De Luca, 2005). However, we found that the primer pair used for this analysis (CrT16H-RT01 and CrRT16H-RT02) was not isoform specific and allowed amplification either of *CYP71D12* or *CYP71D351* depending on source of transcripts. Since *T16H* transcripts detected in leaves are almost exclusively encoded by *CYP71D351 (T16H2)*, we re-investigated the spatial distribution of both transcripts in this organ. By comparing T16H activity in epidermis enriched fraction of leaves obtained by carborundum abrasion versus T16H activity in whole leaves (**Fig. 5A**), we first confirmed that the epidermis hosts most of the corresponding enzymatic activity, as previously described by Murata and De Luca (2005). Quantification of *CYP71D351* expression in the same extracts using isoform specific primers revealed that these gene transcripts followed a similar enrichment in the leaf epidermal fraction (**Fig. 5B**). The carborundum abrasion approach was complemented by localization studies performed by *in situ* RNA hybridization. Using moderate riboprobe hydrolysis and high stringency conditions to distinguish between the two highly similar genes (86.5% nucleotide identity; **Supplemental Figure 1**), no hybridization signals were detected in young leaves using a *CYP71D12*-specific probe (**Fig. 5C-D**). Under the same conditions, *CYP71D351* mRNA was readily detected in adaxial and abaxial epidermis cells (**Fig. 5E-F**).

These results are consistent with the occurrence of four *CYP71D351* ESTs in the *C. roseus* EST epidermome database that were previously incorrectly annotated as *CYP71D12* (**Supplemental Table 1**; Murata et al., 2008) and are also in agreement with the postulated localization of the first two steps of vindoline biosynthesis in the epidermis (Murata and De Luca, 2005; Murata et al. 2008; Guirimand et al., 2011a).

### ***CYP71D351 (T16H2) is an endoplasmic reticulum-anchored enzyme***

Most plant cytochromes P450 characterized to date function as endoplasmic reticulum (ER)-anchored enzymes, as exemplified in *C. roseus* for *CYP71D12*, *CYP72A1* or *CYP76B6* (Guirimand et al., 2009; 2011a; 2011b). However, the recent localization of two carotenoid hydroxylating P450 to plastids (Quinlan et al., 2012) prompted us to analyze the subcellular localization of *CYP71D351* (T16H2). A predictive sequence analysis of this enzyme, which identified a putative 19-residue transmembrane N-terminal helix (residues 4-22; **Supplemental Figure 6**), suggested that *CYP71D351* (T16H2) was a traditional ER-anchored cytochrome P450. The precise subcellular localization of *CYP71D351* was investigated using a C-terminal YFP fusion protein (*CYP71D351*-YFP) that ensured the accessibility of the predicted transmembrane helix located at the N-terminus of the cytochrome P450. In transiently transformed *C. roseus* cells, the fusion protein displayed a fluorescence signal appearing as a network structure surrounding the nucleus and branching all across the cell (**Fig. 6A-D**). This signal also co-localized perfectly with the signal of the “ER”-CFP marker (**Fig. 6E-H**), which indicates that the protein is anchored to ER membrane and probably releases the 16-hydroxytabersonine product in the cytosol according to the classical topology of cytochrome P450s.

### ***CYP71D351 expression correlates with vindoline accumulation in C. roseus cultivars***

Since T16H activity is reduced or missing in the low vindoline-accumulating cultivar Vinca Mediterranean DP Orchid (DP Orchid), the expression levels of *CYP71D12* and *CYP71D351* were analyzed in the young leaves of this cultivar with respect to Little Delicata, a cultivar with an average level of vindoline (Magnotta et al., 2006). Interestingly, *CYP71D351* (T16H2) transcript levels were 4000-fold lower in the Vinca Mediterranean DP Orchid as compared to the Little Delicata cultivar (**Fig. 7**). By contrast, *CYP71D12* (T16H1) transcript levels were similar in both cultivars and also 1000-fold lower than those of *CYP71D351* in Little Delicata. This provides compelling evidence that only expression of *CYP71D351* (T16H2) is directly correlated with foliar vindoline accumulation.

### ***Silencing of CYP71D351 (T16H2) reduces vindoline levels and alters levels of related metabolites***

To confirm the involvement of CYP71D351 (T16H2) in vindoline synthesis in young leaves of *C. roseus*, a virus-induced gene silencing (VIGS) approach was implemented. In our preferred cultivar for VIGS studies, Sunstorm Apricot, foliar transcript levels of *CYP71D12* (T16H1) were below real-time RT-PCR detection levels. However, we designed a specific down-regulation construct for *CYP71D351* including its 3' UTR region, which presented the highest dissimilarity with respect to *CYP71D12* (T16H1) to avoid potential cross-silencing reactions (**Supplemental Figure 1**). Compared to the empty vector control, the *CYP71D351* silencing construct caused a decrease of *circa* 80% of the corresponding transcript in young *C. roseus* leaves (**Fig. 8A**) while CYP71D12 mRNAs still remain below the detection level. We also measured transcript levels of other MIA biosynthetic genes acting both upstream (*G10H*) and downstream (*D4H* and *DAT*) of the T16H step, and found that these were not down-regulated (**Fig. 8A**). Concomitant with the silencing of *CYP71D351*, we observed a reduction in vindoline of about 60% as compared to empty vector controls. Taber sonine levels, on the other hand, were seemingly unaffected (**Fig. 8B**). Further investigation into the metabolite profiles of silenced leaves identified the significant increase of a metabolite with a mass corresponding to that of vindorosine, a leaf alkaloid that is structurally identical to vindoline except for the absence of the methoxy group at the 16 position. Notably, the increase in vindorosine content corresponded roughly to the decrease in vindoline content. Furthermore, putative biosynthetic intermediates in the tabersonine-to-vindoline pathway have been shown to accumulate in *C. roseus* leaves, albeit at low levels (Liscombe et al., 2010). Therefore, we also investigated their fate with respect to the silencing of *CYP71D351*. We observed the significant decrease of a metabolite with the mass of 16-hydroxytabersonine, the direct product of T16H. We also identified metabolites with masses corresponding to those of the last two intermediates in the vindoline and vindorosine pathways, respectively. For the two late vindoline intermediates (desacetoxyvindoline and deacetylvindoline) (**Fig. 1**), a reduction was observed, while for the two late vindorosine intermediates (desacetoxyvindorosine and deacetylvindorosine) an increase was observed. In order to verify the plausibility of our assignment of these metabolites as vindoline/vindorosine pathway intermediates, we carried out an accurate mass analysis of control and silenced leaf extracts, which revealed that the measured masses were within 3 ppm of the theoretical masses of the proposed intermediates (**Supplemental Table 2**).

## **DISCUSSION**

The initial hydroxylation step of tabersonine determines the fate of the aspidosperma alkaloid branch in *C. roseus*. In aerial organs, 16-hydroxylation by T16H directs the flux of tabersonine towards the biosynthesis of vindoline, which is a direct precursor of the valuable dimeric MIAs. In underground organs, hydroxylation at the 19 position by T19H leads to the production of hörhammericine and echitovenine in roots. T19H has recently been cloned and characterized biochemically, and was shown to act stereoselectively on tabersonine and to a lesser extent on lochnericine, an oxygenated tabersonine derivative (Giddings et al., 2011). Recently, the enzymatic characterization of low and high vindoline-accumulating cultivars has revealed the close correlation between T16H activity and vindoline biosynthesis, highlighting the crucial role that T16H plays in controlling the levels of valuable dimeric MIAs (Magnotta et al., 2006). However, no in-depth characterization of T16H has been published since the cloning of a T16H isoform from cell suspension cultures in the late 1990s (Schröder et al., 1999).

Within all tested *C. roseus* organs, young leaves have been shown to possess the highest levels of T16H activity, which mirrors the vindoline accumulation profile (St-Pierre and De Luca, 1995). Interestingly, while not able to synthesize vindoline, *C. roseus* cell cultures also display relatively high levels of T16H activity, and are a convenient system for laboratory studies. Therefore, Schröder and coworkers could readily use cell suspension cultures to clone a T16H isoform (CYP71D12-T16H1) (Schröder et al., 1999). However, there are inconsistencies regarding the *CYP71D12* expression profile in comparison to that of other vindoline biosynthetic genes, especially regarding cellular localization. Most notably, the *16OMT* transcripts that encode the enzyme acting immediately downstream of T16H have been located to leaf epidermis by complementary technical approaches including epidermis enrichment with carborundum abrasion, cell-specific preparation by laser capture microdissection, epidermis EST sequencing, and RNA *in situ* hybridization (Murata and De Luca, 2005; Levac et al., 2008; Murata et al., 2008; Guirimand et al., 2011a). For *CYP71D12*, however, only the first three approaches have suggested epidermal localization, while RNA *in situ* hybridization assays always failed in our hands (unpublished data). These inconsistencies prompted us to clone T16H using *C. roseus* leaves rather than cell suspension cultures as starting material.

The full-length cDNA that we cloned from young leaves encoded a protein sharing 82% identity with CYP71D12 (T16H1), and we named it CYP71D351 or T16H2. Biochemical characterization of recombinant CYP71D12 and CYP71D351 revealed that both enzymes catalyze the regiospecific hydroxylation of tabersonine at the C16-position (**Fig. 2A, Supplemental Figure 3**). Except for the close tabersonine analogues 2,3-dihydro-3-hydroxytabersonine and 2,3-dihydrotabersonine, no other tested compounds were hydroxylated by either of the enzymes, demonstrating a high degree of substrate specificity. In addition, CYP71D351 and CYP71D12 exhibit apparent  $K_m$  values for tabersonine in the nanomolar range ( $70 \pm 20$  nM and  $350 \pm 100$  nM, respectively). Thus, both enzymes have a very high affinity for the tabersonine substrate suggesting a high efficiency of tabersonine hydroxylation *in vivo*. These values are similar to the ones reported for T19H ( $K_m$   $300 \pm 50$  nM; Giddings et al., 2011) but are much lower than the  $K_m$  value initially determined for T16H in crude leaf extracts (11  $\mu$ M), which was established using a T16H-16OMT coupled reaction (St-Pierre and De Luca, 1995). However, since the  $K_m$  value of 16OMT (for 16-hydroxytabersonine) was later shown to be 2.6  $\mu$ M (Levac et al., 2008), it is clear that the initial estimation of the T16H  $K_m$  value for tabersonine was limited by the second step of the coupled assay.

The occurrence of two homologous proteins displaying T16H activity is in agreement with a genomic southern blot analysis carried out using *CYP71D12* (*T16H1*) cDNA as a probe, which suggested the presence of at least two closely related genes for T16H in *C. roseus* (Schröder et al., 1999). Notably, T16H constitutes the only known MIA biosynthetic enzyme encoded by two distinct genes in *C. roseus*. However, the recent availability of massive transcriptomic data from different research groups will make possible a thorough characterization of other biosynthetic genes for homologues. The high level of amino-acid sequence conservation of these two isoforms suggests that they share a common origin with T16H activity and resulted from a relatively recent gene duplication event leading to subfunctionalization or specialization. At this point, not enough orthologs and paralogs from Apocynaceae and related plant species are available to further evaluate the history of this gene duplication. However, relaxation of substrate specificity in CYP71D351 (T16H2) suggests divergent selection pressure compared to CYP71D12 (T16H1). By contrast, T19H, which also hydroxylates tabersonine, displays only 35% identity with both CYP71D12 and CYP71D351 and probably resulted from the recruitment of a phylogenetically distinct P450-encoding gene.

High levels of T16H activity and vindoline production have been previously reported in young leaves (St-Pierre and De Luca, 1995). Even though the biochemical assays indicate that both CYP71D12 and CYP71D351 could potentially be involved in the biosynthesis of vindoline, our analysis of gene expression suggests that CYP71D351 is the major T16H isoform in *C. roseus* leaves, particularly young leaves. Transcripts of *CYP71D12* were only barely detectable in these organs (**Fig. 3B**). The flower-specific expression of *CYP71D12* is surprising, but might reflect either a specialization of this isoform to non-chlorophyllous tissues including etiolated cell cultures, or defense mechanisms dedicated to flowers as observed for pathogenesis-related proteins (Liu and Ekramoddoullah, 2006). The flower bud expression of both *CYP71D351* and *CYP71D12* might also reflect the differential expression of these P450s in chlorophyllous and non-chlorophyllous tissues. Floral synthesis of vindoline reaches 6% of leaf level, and was as expected supported by low levels of *NMT*, *D4H* and *DAT* gene expression in flowers (**Fig. 4, Supplemental Fig. 5**; St-Pierre et al., 1998). These initial observations about the preferential expression of *CYP71D351* in leaves were confirmed by the specific detection of *CYP71D351* transcripts in leaf epidermis, while no *CYP71D12* transcripts were detected anywhere in leaf cross-sections (**Fig. 5A-C**). In addition, the four T16H ESTs annotated as T16H in the *C. roseus* epidermome database (Murata et al., 2008) correspond strictly to *CYP71D351* and not to *CYP71D12* (**Supplemental Table 1**). Therefore, the initial report of *CYP71D12* mRNA within leaf epidermis, obtained by RT-PCR performed on epidermis-enriched RNA extracts, likely resulted from false priming (Murata and De Luca, 2005). Indeed, in our hands, the pair of primers used in this former study to amplify *CYP71D12* leads to amplification of *CYP71D351* from leaf cDNA and is therefore not isoform-specific. Furthermore, the specific expression of *CYP71D351* mRNA in leaf epidermis definitively demonstrates that genes encoding T16H and 16OMT are co-expressed in this tissue. In addition, the anchoring of CYP71D351 to the endoplasmic reticulum, as revealed by subcellular localization studies, most likely exposes the catalytic site towards the cytosol and permits the release of 16-hydroxytabersonine into the cytosol, where 16OMT resides, thus facilitating the following methoxylation reaction (**Fig. 6**, Guirimand et al., 2011a). The comparison of gene expression in low and high vindoline-accumulating cultivars provided further evidence for the key role of CYP71D351 in foliar vindoline biosynthesis. Both types of cultivars were shown to have similar level of activity of vindoline biosynthetic enzymes except for T16H, whose activity is strongly reduced in the low vindoline-accumulating cultivar (Magnotta et al., 2006). Our experiments showed that this deficiency in T16H activity can be directly correlated to the lack of *CYP71D351* transcripts.

Final proof of the crucial role of CYP71D351 (T16H2) in foliar vindoline biosynthesis was provided by downregulation experiments using VIGS. As expected, the downregulation of *CYP71D351* led to a strong decrease of vindoline accumulation. This effect was accompanied by a significant reduction of metabolites with masses corresponding to vindoline pathway intermediates (16-hydroxytabersonine, desacetoxyvindoline and deacetylvindoline). Simultaneously, metabolites with masses related to the vindorosine pathway (deacetoxyvindorosine, desacetylvindorosine, and vindorosine itself) were significantly increased. Vindorosine is the demethoxylated analog of vindoline, and the downstream enzymes NMT, D4H and DAT are known to accept both the 16-methoxylated and the demethoxylated tabersonine derivatives for the production of either vindorosine or vindoline (**Fig. 1** ; De Luca et al., 1987; Liscombe et al., 2010). Therefore, down-regulation of T16H seems to have caused the metabolic flux to be reoriented towards the synthesis of vindorosine rather than towards the production of other MIAs, with no detectable increase of tabersonine (**Fig 8B**). This also implies that the yet unknown enzyme catalyzing the hydration of 16-methoxytabersonine in the vindoline pathway can accept tabersonine as substrate, a fact that might facilitate its discovery.

In conclusion, our results show that CYP71D351 (T16H2) is the main isoform in the biosynthesis of vindoline in *C. roseus* by catalyzing the 16-hydroxylation of tabersonine in young leaves. By contrast, the previously cloned CYP71D12 (T16H1) does not play a role in this foliar biosynthesis and is likely dedicated to the production of vindoline in flowers. Therefore, vindoline biosynthesis is subject to an extraordinary degree of spatial control in *C. roseus*. Such existence of isoforms of MIA biosynthetic enzymes acting in an organ-dependent manner, makes the architecture and regulation of secondary metabolism in *C. roseus* even more complex.

## **MATERIALS AND METHODS**

### ***Plant and cell culture growth***

Mature *C. roseus* (L) G. Don plants, cultivar Pacifica Pink, were used for microscopy fixation (RNA *in situ* hybridization experiments) and RNA extraction (cloning experiments and gene expression measurements in various organs). A low-vindoline accumulating *C. roseus* cultivar (Vinca Mediterranean DP Orchid) and a vindoline-accumulating control cultivar (Little Delicata) (respectively lines 49 and 50 in Magnotta et al., 2006) were used for gene expression analysis. Virus induced gene silencing assays were performed on the *C. roseus*



Sunstorm Apricot cultivar. The *C. roseus* C20D cell suspension culture used for subcellular localization studies and gene expression analysis was propagated in Gamborg B5 medium (Duchefa, NL) at 24°C under continuous shaking (100 rpm) for 7 days as previously described (Guirimand et al., 2009).

### ***RNA extraction and reverse transcription***

For cDNA cloning, extraction of total RNA from young leaves was performed using the NucleoSpin RNA Plant kit (Macherey-Nalgel, France). First-strand cDNA was synthesized from 5 µg of total RNA using oligo(dT)<sub>18</sub> primers (0.5 µM) and 15 units of Thermoscript reverse transcriptase (Invitrogen). Following reverse transcription, complementary RNA was removed by treatment with *E. coli* RNase H (Invitrogen) for 20 min at 37°C. For 5'-rapid amplification of cDNA ends (RACE), similar reactions were carried out except that total RNA was subsequently removed by treatment with RNase A (Sigma-Aldrich) and the reaction product was purified using the NucleoSpin Extract II kit. For real-time PCR, total RNA was extracted from different *C. roseus* organs and cells with RNeasy Plant mini kit (Qiagen) and treated (1.5 µg) with RQ1 RNase-free DNase (Promega) before being used for first-strand cDNA synthesis by priming with oligo(dT)<sub>18</sub> (0.5 µM). Reverse transcription was carried out using Superscript III RT (Invitrogen) at 50°C.

### ***Cloning of CYP71D351***

First rounds of amplification were performed on cDNA obtained by reverse transcription of young leaf RNA, using primers CrT16H-RT01 and CrT16H-RT02 (Primer sequences are described in **Supplemental Table 3**). The amplification product was cloned into the pSC-A plasmid (Stratagene) and fifteen resulting clones were sequenced. On the basis of the resulting sequences and EST sequence analysis, the sense 2T16H-A primer was designed to perform 3'-RACE-PCR according to Oudin et al. (2007). Similarly, the reverse primers 2T16H-51 and 2T16H-52 were used to perform a nested 5'-RACE-PCR as described previously (Guirimand et al., 2012). Following sequence assembly, the two specific primers 2T16H-YFPfor and 2T16H-YFPprev were used to amplify a full length ORF using *Phusion* DNA polymerase (New England BioLabs). The resulting amplicon was cloned into the pSC-A vector following A-tailing and sequenced before deposition at NCBI under Genbank accession number JF742645.

### ***Subcellular localization studies***

To study subcellular localization, the full length CYP71D351 ORF was amplified by PCR using primers 2T16H-YFPfor and 2T16H-YFPprev (**Supplemental Table 3**) and cloned into the *Bgl*II and *Spe*I restriction sites of the pSCA-cassette YFPi plasmid in frame with the 5' extremity of the YFP coding sequence. This recombinant plasmid was used for transient transformation of *C. roseus* cells by particle bombardment and GFP imaging according to Guirimand et al. (2009, 2010a), in combination with plasmids expressing the ER-CFP marker (CD3-954; Nelson et al., 2007) or the nucleus CFP-marker (Guirimand et al., 2011b).

### ***Heterologous expression of CYP71D351 and CYP71D12 in yeast***

Full-length CYP71D12 and CYP71D351 cDNAs were respectively amplified using the primer pairs T16H-*Bgl*II / T16H-*Bgl*IIstop and 2T16H-YFPfor / 2T16H-*Bgl*IIstop (**Supplemental Table 3**), carrying *Bgl*II restriction sites at both extremities, and shifted into the *Bam*HI restriction site of the pYedP60 vector. Both recombinant plasmids as well as the empty vector were independently transformed into the *Saccharomyces cerevisiae* strain WAT11 engineered to express the Arabidopsis NADPH P450 reductase 1 (Pompon et al., 1996). Yeast strains were grown in YPGE medium (1% Bacto Peptone, 1% yeast extract, 0.5% glucose and 3% ethanol) and recombinant expression was induced by glucose starvation in YPI medium (1% Bacto Peptone, 1% yeast extract and 2% galactose) according to Pompon et al. (1996) from a single colony. Cells were harvested by centrifugation and proteins were isolated with microsomal membranes as described in Heitz et al. (2012).

### ***Enzyme assays***

CYP71D351 and CYP71D12 activities, including kinetic parameter determination and substrate specificities, were analysed by UPLC-MS in a final volume of 50  $\mu$ l containing 100 mM Tris-HCl pH 8.0, 4 mM DTT, 1 mM NADPH, various amounts of substrate and 2 or 4  $\mu$ l of microsomes for CYP71D351 and CYP71D12, respectively. The reactions were initiated by addition of NADPH, incubated at room temperature and quenched by the addition of 50  $\mu$ l methanol. Assays without NADPH or with microsomes from yeast harboring the empty expression vector were used as controls. For  $K_m$  and  $V_{max}$  measurements of CYP71D12 and CYP71D351, tabersonine was used at concentrations ranging from 0.12 to 7.5  $\mu$ M and from 0.25 to 3  $\mu$ M, respectively.  $K_m$  and  $V_{max}$  values were calculated from Lineweaver-Burk plots. For substrate specificity determination, enzymatic reactions were carried out at 30°C during 30 min with the following compounds (commercially available or prepared according to De Luca et al. (1987): catharanthine (300  $\mu$ M), vindoline (220  $\mu$ M), ajmalicine (280  $\mu$ M),

secologanin (260  $\mu\text{M}$ ), naringenin (370  $\mu\text{M}$ ) tryptamine (620  $\mu\text{M}$ ), strictosidine (20  $\mu\text{M}$ ), 2,3-dihydroxytabersonine (50  $\mu\text{M}$ ), 2,3-dihydro-3-hydroxytabersonine (50  $\mu\text{M}$ ) and tabersonine (50  $\mu\text{M}$ ). The UPLC chromatography system was coupled to a SQD mass spectrometer equipped with an electrospray ionization (ESI) source controlled by Masslynx 4.1 software (Waters, Milford, MA). Sample separation was performed on a Waters Acquity HSS T3 C18 column (150 mm x 2.1 mm i.d., 1.8  $\mu\text{m}$ ) with a flow rate of 0.4 mL/min at 55°C. 16-hydroxytabersonine was analyzed in ESI<sup>+</sup> mode using the following gradient: from 10:90 to 50:50 acetonitrile/water acidified with 0.1% formic acid over 5 min. The capillary and sample cone voltages were 3,000 V and 30 V, respectively. The cone and desolvation gas flow rates were 60 and 800 Lh<sup>-1</sup>.

### ***CYP71D351 reaction product characterization***

For product characterization, the CYP71D351 enzymatic reaction was performed as described in the previous section (Enzyme assays) but in a final volume of 60 ml containing 2 mg of tabersonine (100  $\mu\text{M}$ ), 50 mg NADPH and 14 ml of microsomes. Following evaporation, the viscous sample (3 ml) was separated into four portions of 750  $\mu\text{l}$ . Each portion was passed through an RP-18 cartridge (500 mg; preconditioned with methanol and water). Each cartridge was flushed with 3 ml water and eluted with 3 ml methanol. The methanol eluates were combined and evaporated to dryness, reconstituted in 1 ml methanol and subjected to HPLC purification using an Agilent HP1100 LC system (Agilent Technologies, Waldbronn, Germany) and a Zorbax SB-C18 column (150 x 4.6 mm i.d., 3.5  $\mu\text{m}$ ) with a flow rate of 1 mL min<sup>-1</sup>. The injected volume was 100  $\mu\text{L}$  per run and the gradient was the following: from 10:90 to 30:70 acetonitrile/water acidified with 0.1% trifluoroacetic acid over 30 min. UV absorption was monitored at 330 nm. The peak at  $R_t$  22.8 min was subjected to NMR analysis. <sup>1</sup>H NMR, <sup>1</sup>H-<sup>1</sup>H COSY, HSQC and HMBC spectra were recorded on an Avance 500 NMR spectrometer (Bruker-Biospin, Karlsruhe, Germany) at 300 K using a 5 mm TCI CryoProbe<sup>TM</sup>. The sample was dissolved in MeOH-*d*<sub>4</sub> (120  $\mu\text{l}$ ) and measured in a 2.5 mm NMR tube. Chemical shifts ( $\delta$ ) are given relative to tetramethylsilane (TMS) as an internal standard and coupling constants are in Hertz (Hz).

### ***NMR data of 16-hydroxytabersonine***

<sup>1</sup>H NMR (500 MHz, MeOH-*d*<sub>4</sub>):  $\delta$  7.32 (1H, d,  $J$  = 8.1 Hz, H-14), 6.53 (1H, d,  $J$  = 2.1 Hz, H-17), 6.37 (1H, dd,  $J$  = 8.1, 2.1 Hz, H-15), 6.05 (1H, d,  $J$  = 10.2 Hz, H-6), 6.00 (1H, dd,  $J$  =

10.2, 4.1 Hz, H-7), 4.21 (1H, d,  $J = 15.8$  Hz, H-8a), 4.01 (1H, brd,  $J = 15.8$  Hz, H-8b), 3.89 (1H, s, H-19), 3.80 (3H, s, OCH<sub>3</sub>), 3.66 (1H, m, H-10a), 3.51 (1H, m, H-10b), 2.92 (1H, d,  $J = 16.7$  Hz, H-4a), 2.31 (1H, d,  $J = 16.7$  Hz, H-4b), 2.16 (2H, m, H<sub>2</sub>-11), 1.23 (1H, m, H-20a), 1.18 (1H, m, H-20b), 0.71 (3H, t,  $J = 7.2$  Hz, H<sub>3</sub>-21).

<sup>13</sup>C NMR (125 MHz, MeOH-*d*<sub>4</sub>):  $\delta$  169.2 (CO), 164.4 (C-2), 160.0 (C-16), 145.9 (C-18), 135.4 (CH-6), 126.5 (C-13), 122.5 (CH-7), 122.4 (CH-14), 108.7 (CH-15), 99.6 (CH-17), 92.6 (C-3), 72.0 (CH-19), 52.6 (C-12), 51.7 (OCH<sub>3</sub>), 51.4 (CH<sub>2</sub>-10), 51.2 (CH<sub>2</sub>-8), 44.4 (CH<sub>2</sub>-11), 41.6 (C-5), 28.5 (CH<sub>2</sub>-4), 27.4 (CH<sub>2</sub>-20), 7.6 (CH<sub>3</sub>-21).

### ***Gene expression analysis (real-time RT-PCR)***

Expression of *CYP71D351*, *CYP71D12*, *G10H*, *16OMT*, *NMT*, *MAT*, *D4H* and *DAT* was analyzed by real-time RT-PCR using the primers described in **Supplemental Table 3**. Depending on experiments, gene expression measurements were performed on reverse-transcribed RNA extracted from different *C. roseus* organs of the Pacifica Pink cultivar (such as roots, first internodes, young and mature leaves, flower buds, flowers, and fruits), young leaves of *C. roseus* of the cultivars Vinca Mediterranean, Little Delicata, and Sunstorm Apricot, epidermis-enriched fraction of young leaves (Little Delicata cultivar) and also from *C. roseus* cells treated during 0.5, 8, 24 or 48 h with 100  $\mu$ M methyljasmonate (MeJa) or mock-treated with ethanol. Real-time PCR was run on a CFX96 Touch Real-Time PCR System (Bio-Rad, Marnes-La-Coquette, France) using the SYBR<sup>®</sup> Green I technology. Each reaction was performed in a total reaction volume of 25  $\mu$ l containing equal amount of cDNAs, 0.2  $\mu$ M forward and reverse primers and 1x SsoAdvanced SYBR Green Supermix (Bio-Rad). The reaction was initiated by a denaturation step at 95°C for 10 min followed by 40 cycles at 95°C for 15 s and 60°C for 1 min. Melting curves were used to determine the specificity of amplifications. Relative quantification of gene expression was calculated according to the  $\Delta\Delta$ Ct method using the 40S ribosomal protein S9 (RPS9) or 60S ribosomal protein as reference genes (**Fig. 4, 5 and 8**). Alternatively, absolute quantification of transcript copy number was performed with calibration curves and normalization with *RPS9* or *60S* reference gene ratios (**Fig. 3 and 7**). In Figures 3, 4, 5 and 7 each assay was performed in triplicate and expression measurements were performed at least twice with independent experimental replicates, though only one experiment is shown. In Figure 8, each assay was performed in duplicate and data correspond to average values of four (for *G10H*, *D4H* and *DAT* expression) or eight (for *CYP71D351* expression) independently silenced plants  $\pm$  SD.

### ***Preparation of epidermis-enriched fractions of C. roseus leaves***

The epidermis of young *C. roseus* leaves was abraded with carborundum to allow RNA extraction and crude protein extract preparation according to Murata and De Luca (2005). *CYP71D351* gene expression was analyzed by real-time RT-PCR and T16H activity was estimated by measuring the amount of 16-methoxytabersonine produced by crude protein extract from the same fractions as described in St-Pierre and De Luca (1995).

### ***RNA in situ hybridization of C. roseus leaves***

The cellular localization of gene transcripts was performed by RNA *in situ* hybridization according to Mahroug et al. (2006). Briefly, full-length ORFs of *CYP71D351* and *CYP71D12* were amplified with *Phusion* DNA polymerase and cloned into the pSC-A plasmid for use in the synthesis of sense and anti-sense digoxigenin-labeled RNA-probes. Paraffin-embedded serial longitudinal sections of young developing leaves were subsequently hybridized with digoxigenin-labeled probes and localized with anti-digoxigenin-alkaline phosphatase.

### ***Virus induced gene silencing (VIGS)***

Due to high sequence identity with *CYP71D12*, the *CYP71D351* silencing fragment was designed in the 3' end and 3'untranslated region (UTR) of the corresponding gene (**Supplemental Figure 1**) and amplified with primers 2T16H fw / 2T16H rev (**Supplemental Table 3**). The resulting fragment (252-bp) was cloned into the pTRV2u vector described in Geu-Flores et al. (2012). The resulting plasmid and the empty vector (EV) were used to perform the VIGS assays on *C. roseus* seedlings as described by Liscombe and O'Connor (2011). Leaves from the first two leaf pairs to emerge following inoculation were harvested from eight plants transformed with each construct and subjected to gene expression analysis by real-time RT-PCR (primers in **Supplemental Table 3**). The alkaloid content of silenced leaves was determined by LC-MS as described previously (Geu-Flores et al. 2012; Liscombe and O'Connor, 2011).

### **ACKNOWLEDGMENTS**

The authors thank Dr. David Nelson (University of Tennessee, Memphis, U.S.A.) for annotation of *CYP71D351*, Dr. Christian Paetz (Max-Planck-Institute for Chemical Ecology, Jena, Germany), Dr. Lionel Hill (John Innes Centre, Norwich, UK) for mass spectrometric analysis and Dr. Renate Ellinger for technical support (Max-Planck-Institute for Chemical

Ecology, Jena, Germany). We also thank M.A. Marquet, M.F. Aury, E. Danos, C. Labarre and E. Marais (EA2106, Tours, France) for help in maintaining cell cultures and plants.

### **LITERATURE CITED**

Burlat V, Oudin A, Courtois M, Rideau M, St-Pierre B (2004) Co-expression of three MEP pathway genes and geraniol 10-hydroxylase in internal phloem parenchyma of *Catharanthus roseus* implicates multicellular translocation of intermediates during the biosynthesis of monoterpene indole alkaloids and isoprenoid-derived primary metabolites. *Plant J* 38:131-141.

De Luca V, Balsevich J, Tyler RT, Kurz WGW (1987) Characterization of a novel N-methyltransferase (NMT) from *Catharanthus roseus* plants. *Plant Cell Rep* 6:458-461

Facchini PJ, De Luca V (2008) Opium poppy and Madagascar periwinkle: model non-model systems to investigate alkaloid biosynthesis in plants. *Plant J* 54:763-784

Geu-Flores F, Sherden NH, Courdavault V, Burlat V, Glenn WS, Wu C, Nims E, Cui Y, O'Connor SE (2012) An alternative route to cyclic terpenes by reductive cyclization in iridoid biosynthesis. *Nature* 492:138-142

Giddings LA, Liscombe DK, Hamilton JP, Childs KL, DellaPenna D, Buell CR, O'Connor SE (2011) A stereoselective hydroxylation step of alkaloid biosynthesis by a unique cytochrome P450 in *Catharanthus roseus*. *J Biol Chem* 286:16751-16757

Gigant B, Wang C, Ravelli RB, Roussi F, Steinmetz MO, Curmi PA, Sobel A, Knossow M (2005) Structural basis for the regulation of tubulin by vinblastine. *Nature* 435:519-522

Guirimand G, Burlat V, Oudin A, Lanoue A, St-Pierre B, Courdavault V (2009) Optimization of the transient transformation of *Catharanthus roseus* cells by particle bombardment and its application to the subcellular localization of hydroxymethylbutenyl 4-diphosphate synthase and geraniol 10-hydroxylase. *Plant Cell Rep* 28:1215-1234

Guirimand G, Courdavault V, Lanoue A, Mahroug S, Guihur A, Blanc N, Giglioli-Guivarc'h N, St-Pierre B, Burlat V (2010a) Strictosidine activation in Apocynaceae: towards a "nuclear time bomb"? *BMC Plant Biol* 10:182

Guirimand G, Courdavault V, St-Pierre B, Burlat V (2010b) Biosynthesis and Regulation of Alkaloids. In *Plant Developmental Biology - Biotechnological Perspectives vol 2* (Pua EC & Davey M, eds), pp. 139-160. Springer Verlag, Berlin Heidelberg.

Guirimand G, Guihur A, Ginis O, Poutrain P, Héricourt F, Oudin A, Lanoue A, St-Pierre B, Burlat V, Courdavault V (2011b) The subcellular organization of strictosidine biosynthesis in *Catharanthus roseus* epidermis highlights several trans-tonoplast translocations of intermediate metabolites. *FEBS J* 278:749-763

Guirimand G, Guihur A, Phillips MA, Oudin A, Glévarec G, Melin C, Papon N, Clastre M, St-Pierre B, Rodríguez-Concepción M, Burlat V, Courdavault V (2012) A single gene encodes isopentenyl diphosphate isomerase isoforms targeted to plastids, mitochondria and peroxisomes in *Catharanthus roseus*. *Plant Mol Biol* 79:443-459.

Guirimand G, Guihur A, Poutrain P, Héricourt F, Mahroug S, St-Pierre B, Burlat V, Courdavault V (2011a) Spatial organization of the vindoline biosynthetic pathway in *Catharanthus roseus*. *J Plant Physiol* 168:549-557

He YL, Chen WM, Feng XZ (1994) Melomorsine, a new dimeric indoline alkaloid from *Melodinus morsei*. *J Nat Prod* 57:411-414

He L, Yang L, Tan R, Zhao S, Hu Z (2011) Enhancement of vindoline production in suspension culture of the *Catharanthus roseus* cell line C20hi by light and methyl jasmonate elicitation. *Anal Sci* 27:1243-1248

Heitz T, Widemann E, Lugan R, Miesch L, Ullmann P, Désaubry L, Holder E, Grausem B, Kandel S, Miesch M, Werck-Reichhart D, Pinot F (2012) Cytochromes P450 CYP94C1 and CYP94B3 catalyze two successive oxidation steps of plant hormone Jasmonoyl-isoleucine for catabolic turnover. *J Biol Chem* 287:6296-6306

Laflamme P, St-Pierre B, De Luca V (2001) Molecular and biochemical analysis of a Madagascar periwinkle root-specific minovincinine-19-hydroxy-O-acetyltransferase. *Plant Physiol* 125:189-198

Levac D, Murata J, Kim WS, De Luca V (2008) Application of carborundum abrasion for investigating the leaf epidermis: molecular cloning of *Catharanthus roseus* 16-hydroxytabersonine-16-O-methyltransferase. *Plant J* 53:225-236

Liscombe DK, O'Connor SE (2011) A virus-induced gene silencing approach to understanding alkaloid metabolism in *Catharanthus roseus*. *Phytochemistry* 72:1969-1977

Liscombe DK, Usera AR, O'Connor SE (2010) Homolog of tocopherol C methyltransferases catalyzes N methylation in anticancer alkaloid biosynthesis. *Proc Natl Acad Sci U S A* 107:18793-18798

Liu JJ, Ekramoddoullah AKM (2006) The family 10 of plant pathogenesis-related proteins: Their structure, regulation, and function in response to biotic and abiotic stresses. *Physiol Mol Plant Pathol* 68: 3–13

Magnotta M, Murata J, Chen J, De Luca V (2006) Identification of a low vindoline accumulating cultivar of *Catharanthus roseus* (L.) G. Don by alkaloid and enzymatic profiling. *Phytochemistry* 67:1758-1764

Mahroug S, Courdavault V, Thiersault M, St-Pierre B, Burlat V (2006) Epidermis is a pivotal site of at least four secondary metabolic pathways in *Catharanthus roseus* aerial organs. *Planta* 223:1191-1200

Murata J, De Luca V (2005) Localization of tabersonine 16-hydroxylase and 16-OH tabersonine-16-*O*-methyltransferase to leaf epidermal cells defines them as a major site of precursor biosynthesis in the vindoline pathway in *Catharanthus roseus*. *Plant J* 44:581-594

Murata J, Roepke J, Gordon H, De Luca V (2008) The leaf epidermome of *Catharanthus roseus* reveals its biochemical specialization. *Plant Cell* 20:524-542

Nelson DR (2006) Cytochrome P450 nomenclature, 2004. *Methods Mol Biol* 320:1-10

Nelson BK, Cai X, Nebenführ A (2007) A multicolored set of in vivo organelle markers for co-localization studies in *Arabidopsis* and other plants. *Plant J* 51:1126-1136

Oudin A, Mahroug S, Courdavault V, Hervouet N, Zelwer C, Rodriguez-Concepcion M, St-Pierre B, Burlat V (2007) Spatial distribution and hormonal regulation of gene products from methyl erythritol phosphate and monoterpene-secoiridoid pathways in *Catharanthus roseus*. *Plant Mol Biol* 65:13-30

Pompon D, Louerat B, Bronine A, Urban P (1996) Yeast expression of animal and plant P450s in optimized redox environments. *Methods Enzymol* 272:51-64



- Quinlan RF, Shumskaya M, Bradbury LM, Beltrán J, Ma C, Kennelly EJ, Wurtzel ET (2012) Synergistic interactions between carotene ring hydroxylases drive lutein formation in plant carotenoid biosynthesis. *Plant Physiol* 160:204-214
- Roepke J, Salim V, Wu M, Thamm AM, Murata J, Ploss K, Boland W, De Luca V (2010) Vinca drug components accumulate exclusively in leaf exudates of Madagascar periwinkle. *Proc Natl Acad Sci U S A* 107:15287-15292
- Schröder G, Unterbusch E, Kaltenbach M, Schmidt J, Strack D, De Luca V, Schröder J (1999) Light-induced cytochrome P450-dependent enzyme in indole alkaloid biosynthesis: tabersonine 16-hydroxylase. *FEBS Lett* 458:97-102
- St-Pierre B, De Luca V (1995) A cytochrome P-450 monooxygenase catalyzes the first step in the conversion of tabersonine to vindoline in *Catharanthus roseus*. *Plant Physiol* 109:131-139
- St-Pierre B, Laflamme P, Alarco AM, De Luca V (1998) The terminal *O*-acetyltransferase involved in vindoline biosynthesis defines a new class of proteins responsible for coenzyme A-dependent acyl transfer. *Plant J* 14:703-713
- St-Pierre B, Vazquez-Flota FA, De Luca V (1999) Multicellular compartmentation of *Catharanthus roseus* alkaloid biosynthesis predicts intercellular translocation of a pathway intermediate. *Plant Cell* 11:887-900
- Sung PH, Huang FC, Do YY, Huang PL (2011) Functional expression of geraniol 10-hydroxylase reveals its dual function in the biosynthesis of terpenoid and phenylpropanoid. *J Agric Food Chem* 59:4637-4643
- Vazquez-Flota F, De Carolis E, Alarco AM, De Luca V (1997) Molecular cloning and characterization of desacetoxyvindoline-4-hydroxylase, a 2-oxoglutarate dependent-dioxygenase involved in the biosynthesis of vindoline in *Catharanthus roseus* (L.) G. Don. *Plant Mol Biol* 34:935-948
- Wenkert E, Cochran DW, Hagaman EW, Schell FM, Neuss N, Katner AS, Potier P, Kan C, Plat M, Koch M, Mehri H, Poisson J, Kunesch N, Rolland Y (1973) Carbon-13 nuclear magnetic resonance spectroscopy of naturally occurring substances. XIX. *Aspidosperma* alkaloids. *J Am Chem Soc* 95:4990-4995

Westekemper P, Wieczorek U, Gueritte F, Langlois N, Langlois Y, Potier P, Zenk MH. (1980) Radioimmunoassay for the determination of the indole alkaloid vindoline in *Catharanthus*. *Planta Med* 39:24-37

### **Figure legends**

**Figure 1. The position of tabersonine hydroxylation governs the biosynthesis of downstream MIAs.** In aerial organs, tabersonine is hydroxylated at the C16 position by tabersonine 16-hydroxylase (T16H) and subsequently metabolized by 16-hydroxytabersonine-16-*O*-methyltransferase (16OMT), uncharacterized hydratase, *N*-methyltransferase (NMT), desacetoxyvindoline-4-hydroxylase (D4H) and deacetylvindoline-4-*O*-acetyltransferase (DAT) to produce vindoline. In roots, tabersonine is hydroxylated at the C19 position by tabersonine 19-hydroxylase (T19H) prior acetylation catalyzed by minovincinine-19-hydroxy-*O*-acetyltransferase (MAT) and additional reactions of reduction or epoxidation. Dashed lines represent uncharacterized enzymatic reactions.

**Figure 2. CYP71D351 and CYP71D12 catalyze the 16-hydroxylation of tabersonine.** (A) LC-MS chromatograms using selected ion monitoring (tabersonine:  $m/z$  337, 16-hydroxytabersonine:  $m/z$  353) of the reaction products of microsomes purified from yeast cell cultures expressing either CYP71D351, CYP71D12 or containing the empty pYeDP60 vector. (B) Partial HMBC spectrum for 16-hydroxytabersonine isolated from yeast culture expressing CYP71D351. The position of the new hydroxyl group was established from HMBC correlations through three bonds (H-14/C-12, H-14/C-16, H-14/C-18, H-15/C-13, H-15/C-17, H-17/C-13 and H-17/C-15) as indicated by arrows in the inserted structure.

**Figure 3. Analysis of CYPD351 (T16H2) and CYP71D12 (T16H1) expression in *C. roseus* organs and cell cultures.** *CYP71D351* (light grey) and *CYP71D12* (dark grey) transcript levels were determined by real-time RT-PCR analyses performed on total RNA extracted from *C. roseus* cells (A) subjected to MeJa- or mock-treatment during 0.5h, 8h, 24h and 48h and from *C. roseus* organs (B). *CYP71D351* and *CYP71D12* transcript copy numbers were normalized using *CrRPS9*. R, roots; S, stem; YL, young leaves; ML, mature leaves; FB, flower buds; Fl, flowers; Fr, fruits.

**Figure 4. CYP71D351 (T16H2) has a similar expression pattern as other vindoline biosynthetic genes.** Relative expression of *CYP71D12*, *CYP71D351*, *16OMT*, *NMT* and *DAT*

were determined by real-time RT-PCR analyses performed on total RNA extracted from various *C. roseus* organs. *MAT*, a root specific hydroxylase, is also included for comparison. *CrRPS9* was used as reference gene. R, roots; S, stem; YL, young leaves; ML, mature leaves; Fl, flowers; FB, flower buds; Fr, fruits.

**Figure 5. T16H activity and *CYP71D351* (*T16H2*) transcripts are specifically located in epidermis of *C. roseus* leaves.** (A) Analysis of T16H enzymatic activity and (B) relative expression of *CYP71D351* in leaf epidermis enriched protein/transcript extracts produced by carborundum abrasion compared with that found in whole leaves. *Cr60S* was used as reference gene. Ep, epidermis; WL, whole leaf. (C-F) Analysis of *CYP71D351* and *CYP71D12* transcript distribution performed by RNA *in situ* hybridization. Serial sections of young developing leaves were hybridized either with *CYP71D12*-antisense (AS) probes (C), with *CYP71D351* AS probes (E), or with *CYP71D12*-sense (S) probes (D) or *CYP71D351* S probes (F) used as negative controls. ab, abaxial epidermis; ad, adaxial epidermis. Bars 100  $\mu\text{m}$ .

**Figure 6. *CYP71D351* (*T16H2*) is located to the endoplasmic reticulum.** *C. roseus* cells were transiently transformed with *CYP71D351*-YFP expressing vector (CYP-YFP; A, E) in combination with plasmids expressing a nucleus-CFP marker (“nuc”-CFP; B) or an endoplasmic reticulum-CFP marker (“ER”-CFP; F). Co-localization of the two fluorescence signals appeared on the merged images (C, G). Cell morphology (D, H) is observed with differential interference contrast (DIC). Bars 10  $\mu\text{m}$ .

**Figure 7. Comparison of *CYP71D351* (*T16H2*) and *CYP71D12* (*T16H1*) transcript levels in low and high vindoline accumulating *C. roseus* cultivars.** *CYP71D12* and *CYP71D351* transcript levels were measured by real-time RT-PCR analyses performed on total RNA extracted from *C. roseus* leaves of the low vindoline accumulating cultivar named DP Orchid (dark grey) and of the high vindoline accumulating cultivar little Delicata (light grey). Transcripts copy number were normalized using the ribosomal 60S RNA.

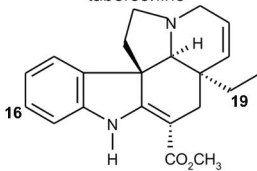
**Figure 8. Down-regulation of *CYP71D351* (*T16H2*) affects vindoline biosynthesis.** (A) *CYP71D351* transcript down-regulation by VIGS. Relative expression of *G10H* (encoding an enzyme involved in secologanin biosynthesis), *CYP71D351*, *D4H* and *DAT* were determined by real-time RT-PCR analyses performed on total RNA extracted from *C. roseus* leaves of *CYP71D351* silenced plants (CYP-VIGS, white bar) or plants transformed with an empty control vector (EV, grey bars). *CrRPS9* was used as a reference gene. Data correspond to

average values (n=4)  $\pm$ SD of independent transformant plants. (B) Relative MIA content in CYP-VIGS plants (white bars) as compared to EV plants (grey bars). The accumulation of tabersonine and 16-hydroxytabersonine (first molecule, R=H and R=OH, respectively), deacetylvindoline and deacetylvindorosine (second molecule, R=H and R=OCH<sub>3</sub>, respectively), vindoline and vindorosine (last molecule, R=H and R=OCH<sub>3</sub>, respectively) was quantified by LC-MS. The amount of each MIA in CYP-VIGS plants was expressed relative to that measured in EV plants (normalized to “1”). Asterisks denote statistical significance (\*, P<0.05; \*\*, P<0.01; \*\*\*, P<0.001 – Student’s *t*-test). The result is representative of eight CYP-VIGS plants and eight EV plants.

**Table I.** *CYP71D351 and CYP71D12 substrate specificities.*  
+ and – denote capacity and incapacity of hydroxylation. Conversion of substrates (%) is given in brackets.

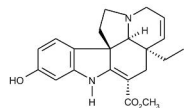
	CYP71D351	CYP71D12
Naringenin	-	-
Tryptamine	-	-
Secologanin	-	-
Strictosidine	-	-
Ajmalicine	-	-
Tabersonine	+++ (96.3±0.6)	+++ (93.6±0.3)
2.3-dihydrotabersonine	+ (31.3±1.7)	+/- (2.1±0.2)
2.3-dihydro-3-hydroxytabersonine	+ (18.2±0.9)	+/- (2.6±0.2)
Vindoline	-	-
Catharanthine	-	-

tabersonine



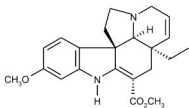
roots

**16-hydroxylation**  
**T16H**



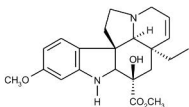
16-hydroxytabersonine

**16OMT**



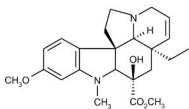
16-methoxytabersonine

**hydratation**



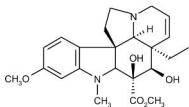
16-methoxy-2,3-dihydro  
3-hydroxytabersonine

**NMT**



desacetoxyvindoline

**D4H**



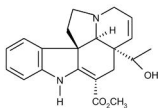
deacetylvindoline

**DAT**



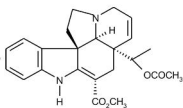
vindoline

**19-hydroxylation**  
**T19H**



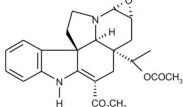
19-hydroxytabersonine

**MAT**



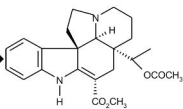
19-O-acetyltabersonine

**6,7-epoxidase**

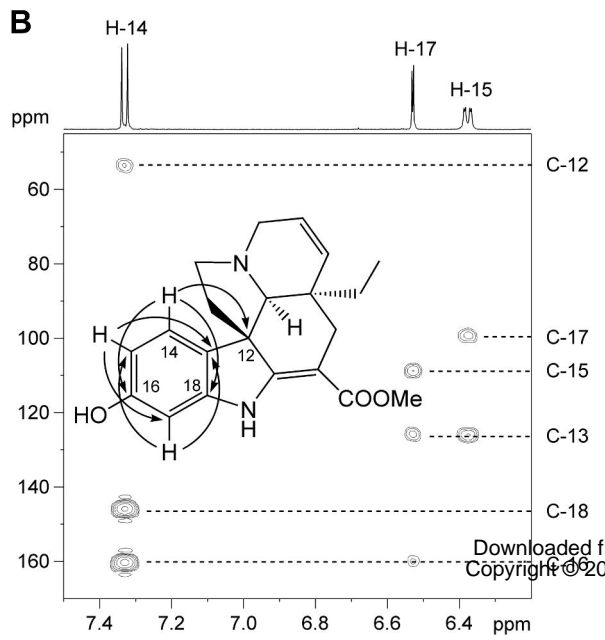
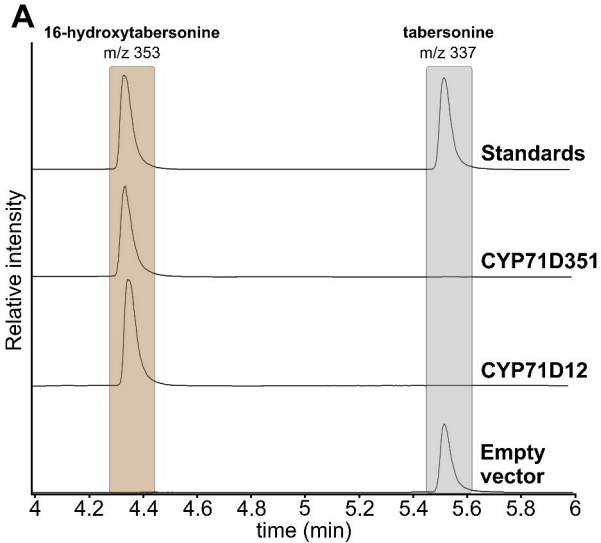


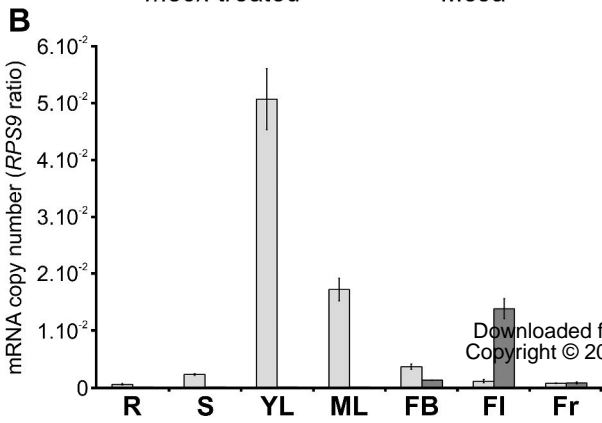
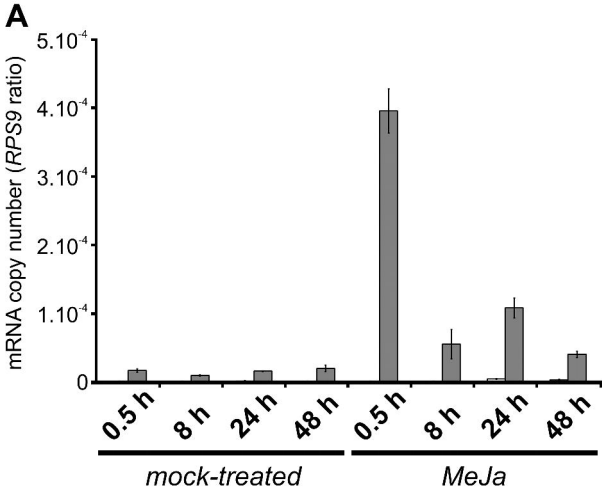
19-O-acetyl  
hörhammericine

**6,7-reductase**

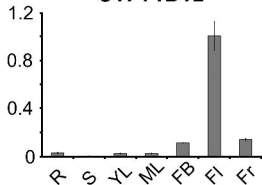
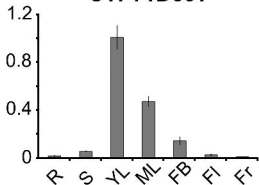
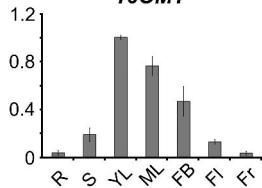
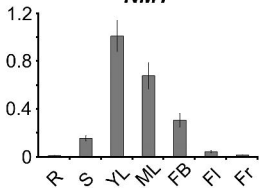
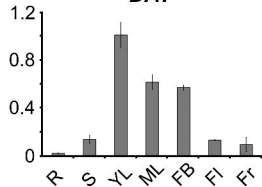
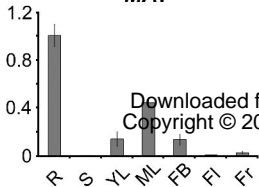


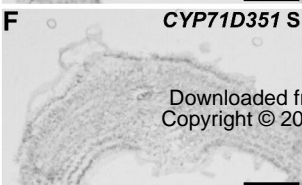
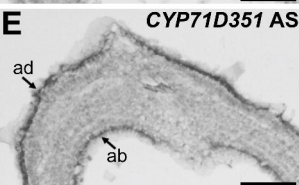
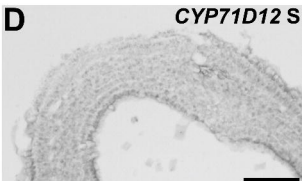
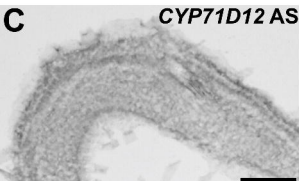
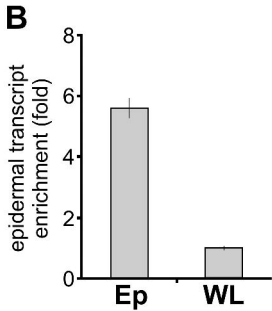
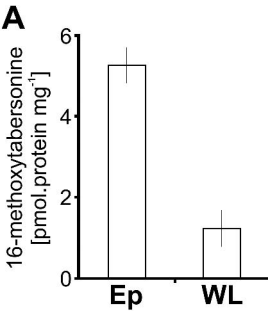
echitovenine

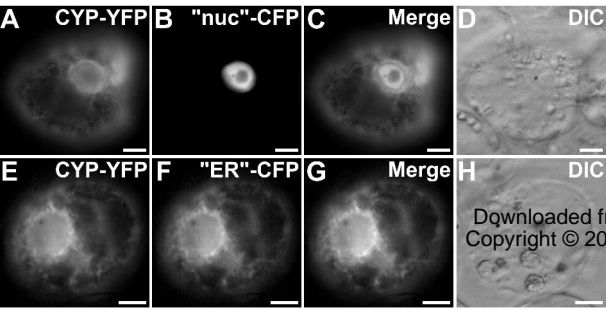


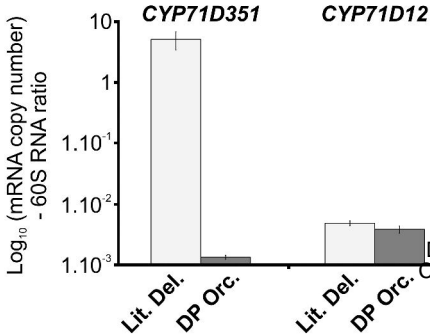


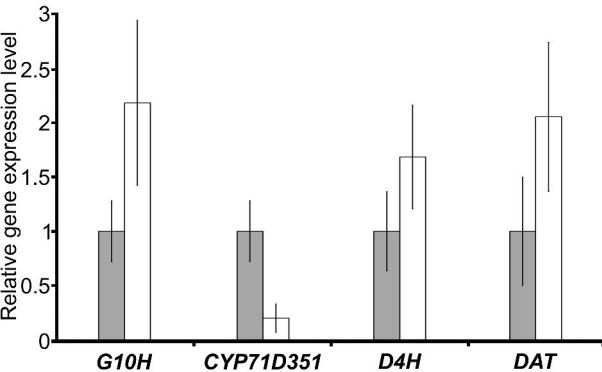


**CYP71D12****CYP71D351****16OMT****NMT****DAT****MAT**







**A****B**